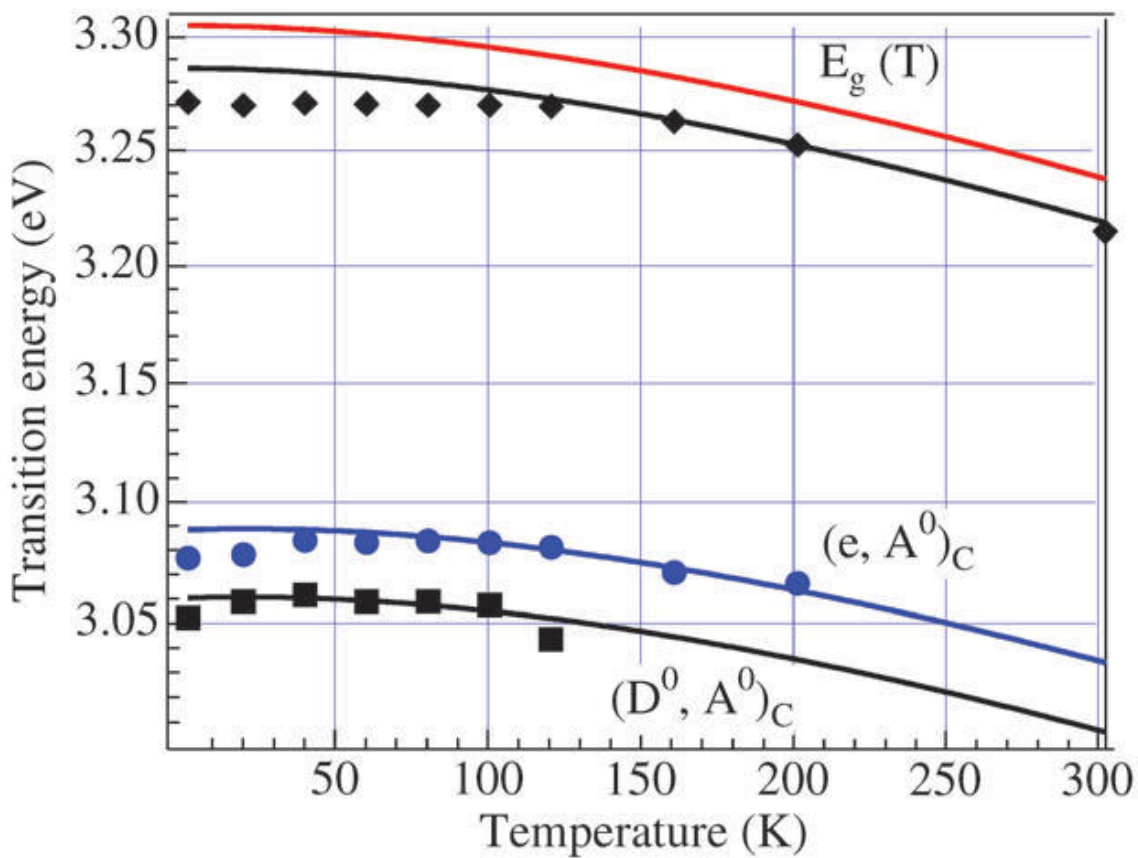


# A Study of Growth and Doping of cubic Group III Nitride Structures



**A Study of  
Growth and Doping  
of  
cubic Group III Nitride Structures**

Dem Department Physik  
der Universität Paderborn  
zur Erlangung des akademischen Grades eines

Doktors der Naturwissenschaften

vorgelegte

**Dissertation**

von

**Ulrich Köhler**

Paderborn, April 2003



# Abstract

Current commercially available advanced optoelectronic devices made from group III Nitrides are based on material exhibiting hexagonal crystal structure. Magnesium is in use as p-type dopant, and Silicon as donor element. Quantum structures make use of ternary and quaternary compositional alloys,  $\text{Al}_x\text{In}_y\text{Ga}_{1-x-y}\text{N}$ , where the Aluminum and Indium mole fractions  $x$  and  $y$ , respectively, allow a precise tailoring of the electronic and structural properties.

Group III Nitrides with cubic crystal symmetry are considered as alternatives because of potentially more favourable material properties. In the course of this thesis work, cubic III Nitrides have been examined in closer detail. Molecular Beam Epitaxy was used to grow GaN and AlN epitaxial films as well as  $\text{Al}_x\text{Ga}_{1-x}\text{N}/\text{GaN}$  heterostructures and quantum structures. Furthermore, cubic Aluminum Nitride was grown both on c-GaN and directly on Gallium Arsenide substrates, thus demonstrating the possibility of direct AlN low temperature nucleation.

The first part of this thesis is concerned with the properties of Carbon as an alternative acceptor in cubic Gallium Nitride. To this purpose Carbon doping sources were constructed and calibrated. By means of temperature-dependent luminescence and Hall measurements the thermal activation energy of Carbon was determined as  $E_A = 215\text{meV}$ . Additionally, excitation-dependent photoluminescence revealed the existence of a Carbon-related deep center. The effect of the incorporation of Carbon in c-GaN was calculated. The experimental results were reproduced by assuming a self-compensation of the Carbon acceptor by a Carbon interstitial. This behaviour explains electrical and optical incorporation-dependent trends.

The second part deals with  $\text{Al}_x\text{Ga}_{1-x}\text{N}$  structures. Electrical measurements revealed p-type conductivity of as-grown samples.  $\text{Al}_x\text{Ga}_{1-x}\text{N}/\text{GaN}$  multi quantum wells were grown and characterized optically and structurally. The energetic positions of the optical QW transitions as a function of well width and barrier Aluminum content were successfully modelled using effective mass theory.



# Contents

Abstract	v
Table of Contents	vii
List of Figures	ix
List of Tables	xi
List of Symbols and Constants	xiii
<b>1 An Introduction</b>	<b>1</b>
<b>2 Fundamentals</b>	<b>5</b>
2.1 GaN, AlN and their Ternaries — A Materials Science View . . . . .	5
2.2 Characterization Techniques . . . . .	8
2.2.1 Luminescence . . . . .	8
2.2.2 Electrical Measurements . . . . .	14
2.2.3 X-ray Diffraction . . . . .	15
2.3 Molecular Beam Epitaxy . . . . .	16
2.3.1 Gallium Nitride Growth . . . . .	18
2.3.2 Gallium Nitride Nucleation . . . . .	19
<b>3 Carbon Doping of GaN</b>	<b>25</b>
3.1 General Considerations . . . . .	26
3.2 Carbon Doping Source . . . . .	28
3.3 Measurements and Results . . . . .	34
3.3.1 Structural Properties . . . . .	34
3.3.2 Photoluminescence . . . . .	37
3.3.3 Electrical Properties . . . . .	43
3.4 Discussion . . . . .	49
<b>4 AlN and AlGaN based Structures</b>	<b>53</b>
4.1 Cubic AlN . . . . .	53
4.1.1 Growth of c-AlN . . . . .	53
4.1.2 Structural Properties of c-AlN . . . . .	54
4.1.3 Further Characterization . . . . .	54

4.2	GaN/AlGaN Quantum Structures . . . . .	55
4.2.1	Modelling Quantum Structures . . . . .	57
4.2.2	Structural Properties . . . . .	60
4.2.3	Luminescence . . . . .	66
4.3	Discussion . . . . .	72
<b>5</b>	<b>Conclusions</b>	<b>75</b>
	<b>Bibliography</b>	<b>79</b>

# List of Figures

2.1	Variation of AlGa <sub>N</sub> gap energy with Aluminum content . . . . .	7
2.2	Schematic of the Photoluminescence setup . . . . .	10
2.3	Schematic of the PL apparatus additon . . . . .	11
2.4	Typical GaN reflection spectrum . . . . .	12
2.5	Schematic of the Cathodoluminescence setup . . . . .	13
2.6	Electron beam penetration depths over acceleration voltage . . . . .	14
2.7	Schematic of the materials research diffractometer . . . . .	16
2.8	Schematic of an MBE system . . . . .	17
2.9	Quadrupole mass spectrum over 0–200amu. . . . .	18
2.10	Detail of a Quadrupole mass spectrum. . . . .	19
2.11	(002) rocking curve widths <i>vs.</i> Ga flux and time . . . . .	20
2.12	(002) rocking curve widths of nucleation processes . . . . .	21
2.13	PL exciton linewidths for different nucleation processes . . . . .	22
2.14	Substrate coverage during nucleation . . . . .	23
3.1	Comparison of acceptor energy trends in III–V semiconductors . . . . .	27
3.2	Graphite vapour pressure and atom flux . . . . .	28
3.3	Head of the $e^-$ -flux cell . . . . .	29
3.4	Detailed view of $e^-$ -flux cell filament . . . . .	30
3.5	Total of $e^-$ -flux cell . . . . .	31
3.6	Filament cell before assembly . . . . .	32
3.7	Filament graphite cell . . . . .	33
3.8	Carbon flux calibration curve. . . . .	34
3.9	Quadrupole Carbon measurements . . . . .	35
3.10	X–ray scans of a c–GaN:C sample . . . . .	36
3.11	AFM scans of c–GaN:C samples . . . . .	37
3.12	PL spectra of c–GaN samples with different Carbon doping . . . . .	38
3.13	Variation of Carbon–related PL with C flux . . . . .	39
3.14	Ratio of C–related to near–edge intensity . . . . .	40
3.15	Photoluminescence spectra taken at different temperatures . . . . .	41
3.16	Temperature shift of near band edge Photoluminescence . . . . .	42
3.17	PL intensity of c–GaN:C as function of excitation intensity . . . . .	43
3.18	Hall data as a function of Carbon incorporation . . . . .	44
3.19	Self–compensation model and comparison to Hall data . . . . .	47
3.20	Temperature–dependent Hall data . . . . .	48
3.21	Carbon incorporation model verified by hole concentration and PL . . . . .	50

4.1	RHEED image of an AlN sample . . . . .	54
4.2	(113) reciprocal space map of cubic AlN on c-GaN . . . . .	55
4.3	GaN/Al <sub>x</sub> Ga <sub>1-x</sub> N MQW sample layout . . . . .	56
4.4	RHEED image of GaN/Al <sub>x</sub> Ga <sub>1-x</sub> N MQW sample after growth stop . . . . .	57
4.5	Transmission spectrum of a c-Al <sub>x</sub> Ga <sub>1-x</sub> N structure on c-GaN . . . . .	58
4.6	Critical thickness of cubic Al <sub>x</sub> Ga <sub>1-x</sub> N layers on c-GaN . . . . .	59
4.7	Schematic of the energetics of a GaN/Al <sub>x</sub> Ga <sub>1-x</sub> N quantum well . . . . .	60
4.8	RSM of the (113) reflex of a GaN/Al <sub>0.08</sub> Ga <sub>0.92</sub> N MQW sample . . . . .	61
4.9	RSM of a GaN/AlGaN MQW sample showing no strain . . . . .	62
4.10	$\omega - 2\theta$ scan of (002) GaN/Al <sub>0.24</sub> Ga <sub>0.76</sub> N MQW reflex . . . . .	63
4.11	TEM image of fivefold GaN quantum well . . . . .	64
4.12	TEM image of GaN MQWs with atomic resolution . . . . .	65
4.13	TEM image of GaN multi quantum well . . . . .	66
4.14	Fluctuation of QW and barrier thickness . . . . .	67
4.15	Variation of QW and barrier thickness in growth direction . . . . .	68
4.16	AFM images of MQW sample . . . . .	69
4.17	Depth-resolved RT CL spectra of 2.5/5nm MQW sample . . . . .	70
4.18	Ratio of quantum well to Al <sub>0.24</sub> Ga <sub>0.76</sub> N bulk luminescence intensity . . . . .	71
4.19	CL spectra of 5x and 20x GaN/Al <sub>x</sub> Ga <sub>1-x</sub> N MQW samples . . . . .	72
4.20	Variation of QW luminescence energy with well width and barrier height . . . . .	73
4.21	Comparison of QW model with CL peak energies . . . . .	74

# List of Tables

2.1	Summary of published data, calculated for cubic GaN. . . . .	6
2.2	Summary of published data, calculated for cubic AlN. . . . .	6
3.1	Data of the Carbon acceptor in c-GaN from optical measurements . . .	40
3.2	Electrical data of the Carbon acceptor in c-GaN . . . . .	48
4.1	Published experimental values of $a_0$ and $E_g$ for c-AlN . . . . .	53
4.2	Summary of electrical data for cubic AlN. . . . .	54
4.3	Summary of TEM data for 5nm/10nm GaN/Al <sub>0.24</sub> Ga <sub>0.76</sub> N MQW structure	65
4.4	CL intensity of GaN/Al <sub>x</sub> Ga <sub>1-x</sub> N MQW samples . . . . .	70



# List of abbreviations

AFM	<i>Atomic Force Microscope/Microscopy</i>
BEP	<i>Beam Equivalent Pressure</i>
CL	<i>Cathodoluminescence</i>
cw	<i>Continuous Wave</i>
DFT	<i>Density Functional Theory</i>
DOS	<i>Density of States</i>
EDX	<i>Energy Dispersive X-Ray Analysis</i>
EL	<i>Electroluminescence</i>
ELOG	<i>Epitaxial Lateral Overgrowth</i>
FWHM	<i>Full Width at Half Maximum</i>
HRXRD	<i>High-Resolution X-Ray Diffraction</i>
HVPE	<i>Halide Vapour Phase Epitaxy</i>
IR	<i>Infrared</i>
LD	<i>Laser Diode</i>
LDA	<i>Linear Density Approximation</i>
LED	<i>Light Emitting Diode</i>
LT	<i>Low Temperature</i>
MBE	<i>Molecular Beam Epitaxy</i>
MOCVD	<i>Metal-Organic Chemical Vapour Deposition</i>
MOVPE	<i>Metal-Organic Vapour Phase Epitaxy</i>
MQW	<i>Multi Quantum Well</i>
PBN	<i>Pyrolytic Boron Nitride</i>
PG	<i>Pyrolytic Graphite</i>
PL	<i>Photoluminescence</i>
PMT	<i>Photomultiplier Tube</i>
QMS	<i>Quadrupole Mass Spectrometer</i>
QW	<i>Quantum Well</i>
rf	<i>Radio Frequency</i>
RHEED	<i>Reflection High Energy Electron Diffraction</i>
RSM	<i>Reciprocal Space Map</i>
RT	<i>Room Temperature</i>
SEM	<i>Scanning Electron Microscope/Microscopy</i>
SIMS	<i>Secondary Ion Mass Spectrometry</i>
SL	<i>Superlattice</i>
STM	<i>Scanning Tunneling Microscope/Microscopy</i>
TEM	<i>Transmission Electron Microscope/Microscopy</i>
UHV	<i>Ultra-High Vacuum</i>
UV	<i>Ultraviolet</i>
VT	<i>Variable Temperature</i>
XRD	<i>X-Ray Diffraction</i>